Experimental evaluation of a needle-to-grid EHD pump prototype for semiconductor cooling applications

Emmanouil D. Fylladitakis
Electronic & Computer Engineering Department
Brunel University London
Middlesex, UB8 3PH, UK
Emmanouil.Fylladitakis@brunel.ac.uk

Antonios X. Moronis, Konstantinos N. Kiousis
Department of Energy Technology
Technological Educational Institute (TEI) of Athens
Aegaleo 12210, Greece
amoronis@teiath.gr / konstantinosq@gmail.com

***Abstract*—A parametric study of a single needle-to-grid EHD air pump, intended for semiconductor cooling applications, is being presented in this paper. The effect of the distance between the emitter and collector electrodes, as well as the radius of the collector's grid wires, is being examined. To that end, several experimental EHD pump prototypes have been fabricated and their performance has been investigated. The experiments demonstrate that this simple and low-cost design is capable of producing usable results, depending on the space and voltage restrictions of the application, for emitter to collector distances greater than 15 mm.**

***Keywords*—EHD pump, needle to grid, electrohydrodynamics, forced convection cooling, ionic wind**

I. Introduction

Ever since the early 17th century, Niccolo Cabeo observed an air flow between two asymmetric high voltage electrodes, which was later recorded by Francis Haukbsee[1]. Even though the phenomenon was observed and recorded, scientists lacked the knowledge to fully explain it for centuries, with the first quantitative analysis taking place in 1899[2].

Today, electrohydrodynamic (EHD) effects are accepted as the result of a high electric potential difference across a pair (emitter – collector) of electrodes having substantially different radii of curvature [3, 4]. Such configurations under specific conditions may generate ionic wind, which has been related to the corona discharge current flowing between a high voltage emitter of small dimensions and a large collector at zero potential [5].

Even though the phenomenon has been observed several centuries ago, its complexity prevented scientists from fully explaining it and exploring its practical potential. Even though it is possible to simplify the mathematical problem when proper boundary conditions are set, the mathematics for solving the problem for more than one practical problem have not yet been developed [6]. However, due to the advancement of modern computers and computational methods capable of solving such problems [7], the interest on researching and analyzing the EHD phenomena has been resurfaced.

The recent advancements on the analysis of the EHD phenomenon of the past several years have sprung a significant interest over the potential practical applications the EHD effect, with most of the research taking place being particularly focused on thrust [8-12] and fluid pumping applications [13-17]. Significant research is also taking place regarding the performance of unexplored electrode configurations [18, 19] and the optimization of the EHD flow characteristics [20, 21].

In this paper, a parametric analysis of a single needle (emitter) to grid (collector) has been performed, with the intention of being used as an air pump for active cooling applications, such as cooling of high power density microelectronic processors. The particular configuration has been chosen due to the strong inhomogeneous field which it generates and its very simple fabrication process.

II. Experimental Setup

A. Electrode geometry

This study is focused on the performance of a single needle to grid configuration, with the needle (emitter) always connected to a constant positive potential (high voltage) and the grid (collector) permanently connected to ground. This configuration creates a very strong

inhomogeneous electric field [20, 22, 23], which is vital to the generation of EHD flow, since the EHD effect is directly connected with the onset of the corona discharges and the production of ionic wind [24]. Ionic wind is created as charged ions collide with the air molecules and atoms while moving from the emitter to the collector, thus transferring their momentum and generating an airflow [25, 26]. As this configuration is meant to be used in an active cooling configuration for a high power density electronic apparatus, we fabricated the prototype with an internal diameter D of 74mm, a feasible replacement for 80mm cooling fans which are commonly used in electronic equipment today. A 316L steel needle with a tip radius r of 32μm is being used as an emitter electrode, while a 316L steel grid with a wire radius R of 560μm and a nominal aperture of 61% is being used as a collector electrode. Fig. 1 displays a 2D schematic of the configuration, where the critical geometrical parameters D, d, r and R of the selected electrode configuration is shown.

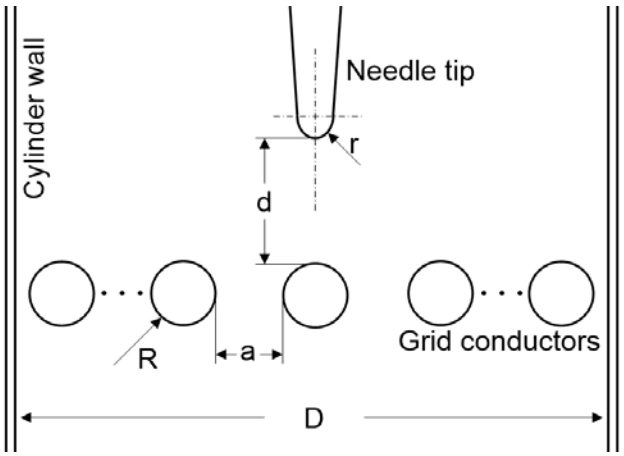

Fig. 1. 2D schematic of the needle to grid EHD pump configuration examined in this paper

B. Experimental equipment

The required high voltage for the initiation of the EHD phenomena and thus the generation of the ionic wind was supplied by an adjustable high voltage power source (Matsusada Precision W Series). A Norma LP10 multimeter combined with a Coline HV40B 1000:1 high voltage probe have been used for measuring the voltage applied to the prototypes, with an accuracy of 1%. Current readings (corona current) have been acquired by a Thurlby 1503 high precision ammeter with 1nA sensitivity. An RTM AM-4836V Anemometer (2% accuracy) has been adapted at the outlet of the pump, at a fixed distance of 3cm away from the grid, for measuring the exit air wind speed and volume. Its axis had been aligned with the wind flow direction. The experimental setup and measuring equipment which has been used for the experimental evaluation of the pump prototypes is shown in Fig. 2.

III. Results and Discussion

A. Influence of the electrode gap d

In order to examine the practical effect of the electrode gap d, experiments have been performed on gaps between 5mm and 50mm. At 5mm the generated electric field was too uniform and the space between the electrodes too short for the EHD phenomenon to expand fully, therefore the generated airflow was insignificant and virtually without practical application.

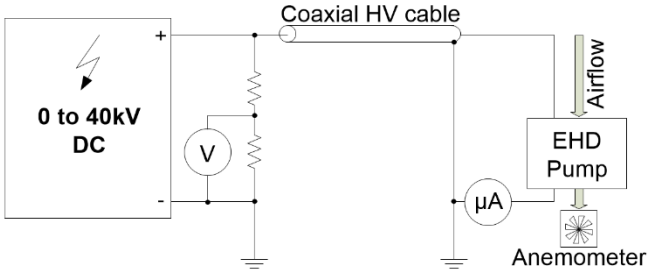

Fig. 2. Experimental setup and measuring equipment configuration

At 50mm, the required high voltage potential to achieve workable results was very high, negating the possibility of using such a device for immediate practical applications. Thus, thorough experiments have been performed with electrode gaps of d_1=10mm, d_2=15mm, d_3=20mm, d_4=25mm, d_5=30mm and d_6=40mm. Fig. 3 displays the corona current of all six configurations, from the point where the phenomenon generates workable airflow to the breakdown limit of the electrode gap d in each configuration.

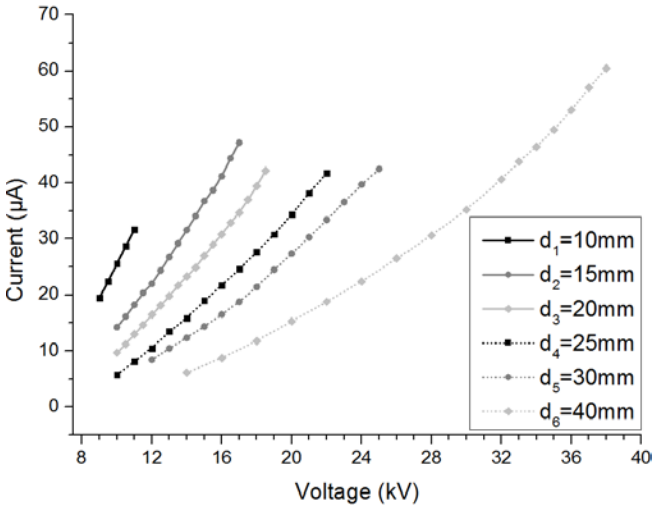

Fig. 3. Corona current of the single needle EHD pump prototypes for different gap distances d

The efficiency n of the EHD apparatus is being described by Eq. 1:

$$n = \frac{\frac{1}{2} \cdot \rho \cdot A \cdot U^3}{V \cdot I} \cdot 100\% \quad (1)$$

Where ρ is the density of the air at the time of the experiment, A is the cross surface area of the circular duct, U is the wind speed velocity, V is the voltage potential applied to the emitter and I is the corona current. During the experiments, the temperature was ranging between 22 and 24°C, the atmospheric pressure was constant at 1014.3 hPa

and the relative humidity was ranging between 32% and 36%. As the breakdown limit is mainly affected by the atmospheric pressure and temperature, the operational limits of the proposed configurations may be only slightly altered, depending on the climatic conditions in the area of the application, as can be estimated by the correction factor related to air density (Eq. 2)[27, 28].

$$\delta = \frac{p}{p_0} \times \frac{T_0}{T} \quad (2)$$

Where p_0 is the air pressure of standard condition, p is the air pressure at test conditions,t_0=20°C and t is the temperature in °C at test conditions.

Fig. 4 displays the efficiency and exit wind speed of the first single needle EHD prototype, with an electrode gap of 10mm. Due to the small electrode gap, the operational voltage range is very narrow; therefore, the exit wind speed is low but measurable. The efficiency of the apparatus also is very low, maxing out at 0.078%.

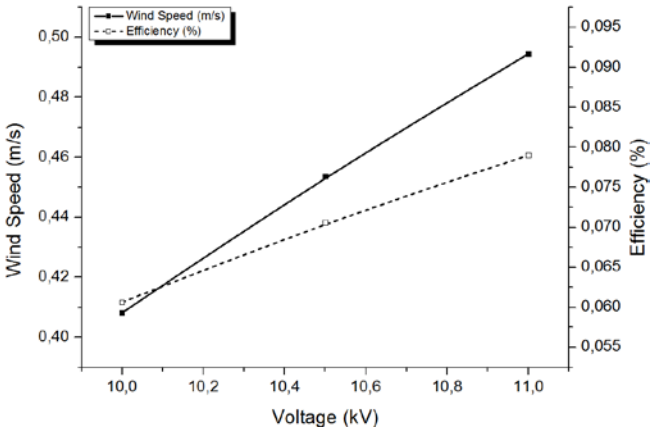

Fig. 4. Exit wind velocity and efficiency of the prototype EHD pump, electrode gap d = 10mm

When the electrode distance is increased to 15mm, as displayed in Fig 5, the operational voltage range becomes much wider, which allows for greater wind speeds and safer operation.

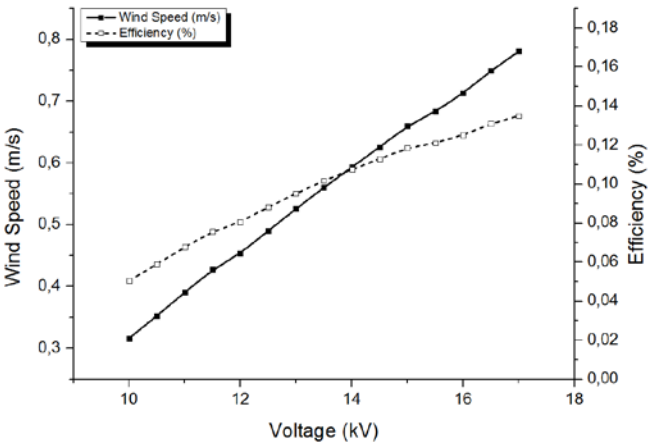

Fig. 5. Exit wind velocity and efficiency of the prototype EHD pump, electrode gap d = 15mm

Still, the maximum efficiency remains low, at 0.133% just before the breakdown limit. The low efficiency however also is a derivative of the large diameter of the apparatus. According to previous work with a similar configuration and a voltage of about 12kV [20], a needle to grid pump with a diameter of 20mm generated an air flow of about 1.5CFM, while the device described in this study generates a flow of 4.1CFM, which is higher.Fig. 6 displays the behavior of the EHD prototype with an electrode gap distance of 20mm. The operational voltage range increases slightly and the exit wind per kV is nearly the same as that of the apparatus with an electrode gap distance of 15mm; however, the efficiency of the prototype increases significantly, especially across the middle of the voltage range.

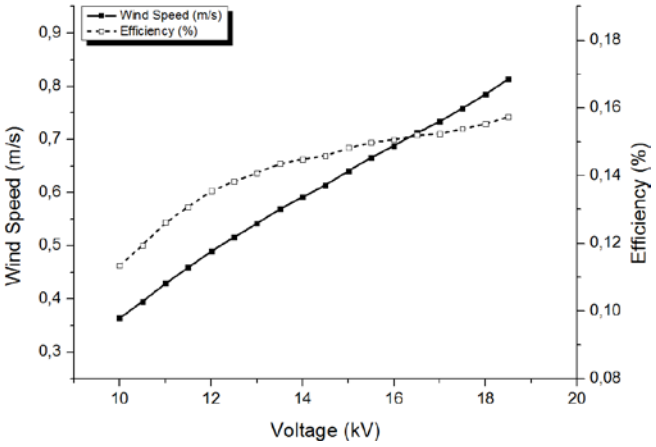

Fig. 6. Exit wind velocity and efficiency of the prototype EHD pump, electrode gap d = 20mm

Increasing the electrode gap to 25mm (Fig. 7) and to 30mm (Fig. 8) again indicates that the device should be capable of producing similar airflow per kV, yet the operational range increases and the efficiency improves significantly. For instance, when a voltage of 18kV is applied to the emitter, the exit wind speed of the prototypes with an electrode gap distance between 20mm and 30mm is about 0.75m/s; however, the efficiency improves from 0.155% at 20mm, to 0.195% at 25mm and then to 0.245% at 30mm.

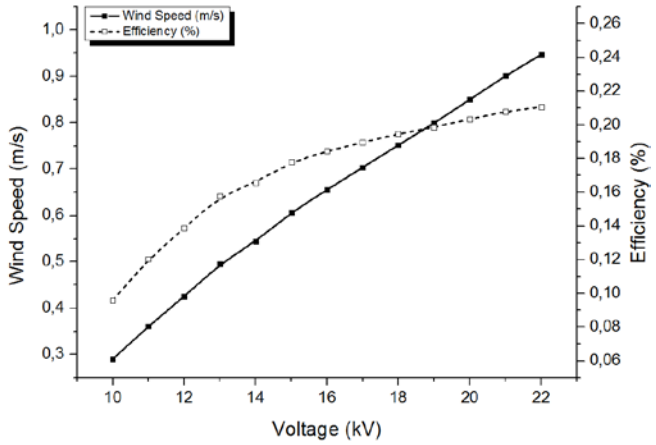

Fig. 7. Exit wind velocity and efficiency of the prototype EHD pump, electrode gap d = 25mm

The breakdown voltage of the prototype with an electrode gap at 30mm is much higher than 18kV as well, meaning that the device is less susceptible to random breakdowns under these specific operational conditions. According to bibliography [29], over a similar electrode distance, a wire to cylinder configuration, a voltage of 14kV and a diameter of 20mm an airflow of about 2.1CFM has been generated without the aid of a negative corona and 2.6CFM with a -8kV supportive wire electrode, while the simple device described in this paper generates 5.1CFM.

A further increase of the electrode gap distance to 40mm vastly increases the operational voltage range of the experimental apparatus, with the breakdown point reaching up to 39kV. As Fig. 9 denotes, the experimental EHD pump is capable of producing significantly greater exit wind speeds and the efficiency improves as the voltage applied to the emitter increases further.However, the performance at lower voltages decreases and a voltage exceeding 30kV is required for the apparatus to deliver high performance, which may be forbidding for most practical applications.

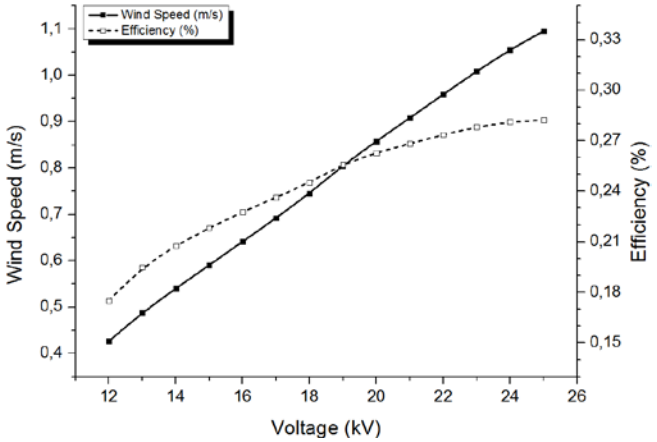

Fig. 8. Exit wind velocity and efficiency of the prototype EHD pump, electrode gap d = 30mm

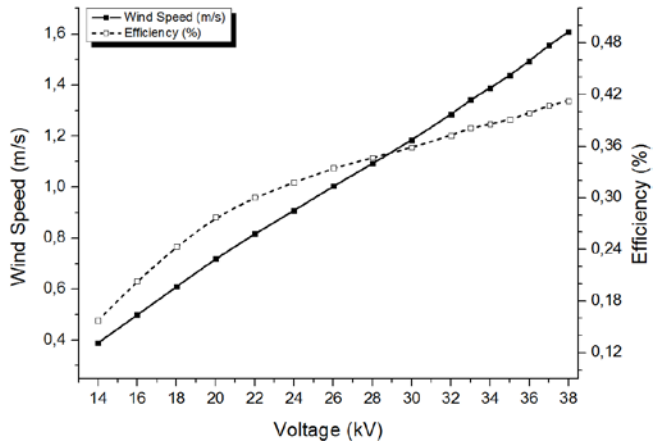

Fig. 9. Exit wind velocity and efficiency of the prototype EHD pump, electrode gap d = 40mm

This configuration, albeit the very high voltage needed to operate, manages to boost the efficiency of the configuration up to a maximum of 0.415% before the breakdown point. Furthermore, the efficiency at lower operational voltages is higher than that of the other configurations, surpassing for example the efficiency of the prototype with an electrode gap of 25mm by 0.09% at 22kV, a 40% increase in efficiency. At the same time, the airflow remains the same and the breakdown limit of the prototype with an electrode gap of 40mm is much higher than that voltage point, while the prototype with an electrode gap of 25mm is operating near its limit.

Fig. 10 displays the airflow produced by each of the aforementioned experimental EHD pumps. It can be seen that a higher voltage needs to be applied in order to produce the same level of airflow over an increased electrode distance; however, for an increasing electrode distance, the operational voltage range of the EHD pump widens as well, ultimately allowing the experimental apparatus to generate greater airflow. This however is susceptible to the maximum voltage allowed for each application.

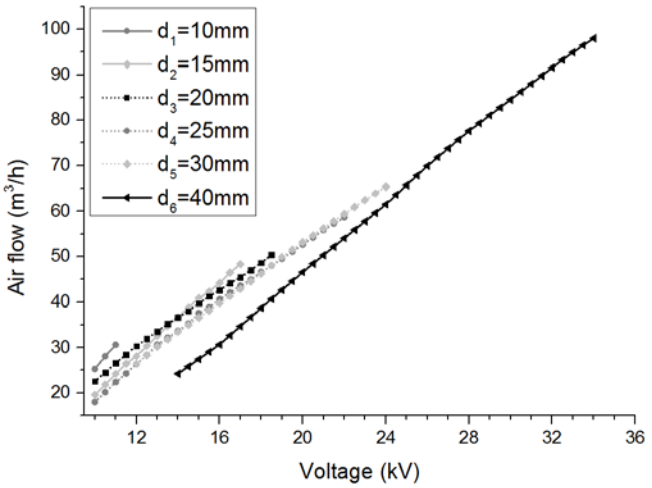

Fig. 10. Air Flow generated by the experimental EHD pump configurations.

B. Influence of the collector grid wire radius R

In order to assess the effect of the collector grid wire radius R, the collector grid has been replaced with a 316 steel grid with a wire radius R of 200μm and a nominal aperture of 81.8%. The higher aperture of the grid should reduce the pressure drop at higher exit velocities.

Our experiments displayed that the actual performance difference is insignificant at wind speeds lower than 0.75m/s and when a relatively low voltage is applied to the emitter, meaning that the replacement of the collector grid held no practical meaning for most of the single needle experimental EHD pumps used in this study, which cannot achieve such an exit wind speed at all or only near the breakdown limit. Fig. 11 displays the difference in exit wind speed and efficiency of the sixth prototype, with an electrode gap distance of 40mm. The larger aperture of the 200μm grid allows the experimental device to achieve higher wind speeds while the rise of the corona current is small (Fig. 12),

thus increasing the efficiency of the single needle EHD pump. The increase of the corona current suggests that the smaller radius R of the grid collector wires increases the inhomogeneity of the electric field, thus enhancing ionic wind and the generated EHD flow.

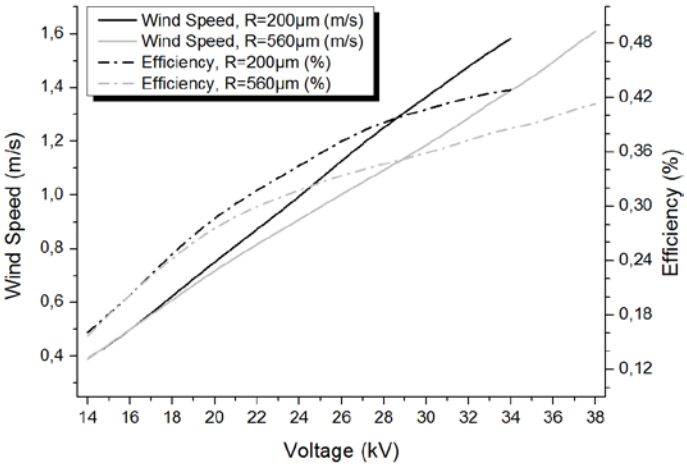

Fig. 11. Exit wind velocity and efficiency of the sixth EHD pump prototype utilizing collector grids of different radiuses R.

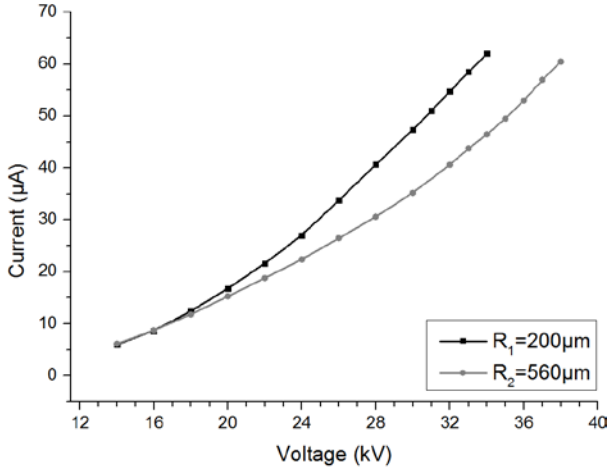

Fig. 12. Corona current of the single needle EHD pump prototype with an electrode gap d=40mm.

On the other hand, this also makes the apparatus less stable at highervoltage levels, in terms of reducing the breakdown voltage limit. Nevertheless, the performance and efficiency enhancement is significant once the voltage applied to the emitter reaches 20kV, far from the breakdown limit which, even though it decreased, it now is at 34kV. This could improve the feasibility of using a single needle to grid EHD pump design with an electrode gap distance of 40mm for air pumping applications if a voltage between 20kV and 30kV can be applied to the emitter.

IV. Conclusion

As it can be derived from the experimental results, the efficiency of the single needle to grid EHD pump improves significantly as the electrode gap d increases while maintaining the same voltage applied to the emitter. The average exit wind speed is negatively affected by increasing the electrode gap distance d while maintaining the same voltage applied to the emitter, yet clearly not significantly enough so as to justify the multiplication of efficiency and the increase in stability.

Single needle to grid EHD pumps appear capable of producing satisfactory results with a voltage of about 14kV applied to the emitter and an emitter to collector distance of 20mm. As the distance increases, so does the operational range and the maximum possible output of the experimental device; however, a significantly higher voltage is required, therefore the practical applications are limited by the high voltage required for the device to operate.

The selection of a grid with a smaller wire radius R offers insignificant performance improvements at smaller electrode gaps and relatively low voltages. Still, the reduction of the collector grid radius R offers very significant performance improvements over large electrode gaps distances, when the applied voltage and exit wind speeds are high, as it both creates a less homogeneous electric field which enhances the EHD phenomenon and the greater aperture is less restrictive towards the flow. However, an emitter voltage of over 20kV is required to justify the use of such a grid due to the distance between the emitter and collector electrodes, which may be too high for compact practical applications.

Finally, the results of this study indicate that the performance of a single needle to grid EHD pump prototype may reach levels usable for practical forced convection cooling applications such as cooling of semiconductors in consumer electronics etc. Despite the extra cost of the high voltage power supply, it could become a viable replacement of mechanical fans, considering the great simplicity of the design and the noiseless operation, which, in some cases may be a necessity.

References

[1] M. Robinson, "A history of the electric wind," *American Journal of Physics*, vol. 30, p. 366, 1962.

[2] A. P. Chattock, "On the velocity and mass of the ions in the electric wind in air," *Philosophical Magazine*, vol. 48, pp. 401-420, 1899.

[3] J. S. E. Townsend, *Electricity in gases*. Oxford: Clarendon Press, 1915.

[4] L. B. Loeb, *Electrical coronas*. London: University of California Press, 1965.

[5] E. Lob, *Archiv der elektrischen Uebertragung 8*, 1954.

[6] R. D. Morrison and D. M. Hopstock, "The distribution of current in wire-to-cylinder corona," *Journal of Electrostatics*, vol. 6, pp. 349-360, 1979.

[7] J. P. A. Bastos and N. Sadowski, *Electromagnetic Modeling by Finite Element Methods*: Taylor & Francis, 2003.

[8] D. Kirtley and J. M. Fife, "Modeling, simulation, and design of an electrostatic colloid thruster," in *Plasma Science, 2002. ICOPS 2002. IEEE Conference Record - Abstracts. The 29th IEEE International Conference on*, 2002, p. 174.

[9] Z. Lin and L. Teck-Meng, "Thrust origin in EHD lifters," in *Industry Applications Society Annual Meeting (IAS), 2011 IEEE*, 2011, pp. 1-5.

[10] L. Pekker and M. Young, "Model of Ideal Electrohydrodynamic Thruster," *Journal of Propulsion and Power*, vol. 27, pp. 786-792, 2011.

[11] L. F. Velasquez-Garcia, A. I. Akinwande, and M. Martinez-Sanchez, "A Planar Array of Micro-Fabricated Electrospray Emitters for Thruster Applications," *Microelectromechanical Systems, Journal of*, vol. 15, pp. 1272-1280, 2006.

[12] L. F. Velasquez-Garcia, A. I. Akinwande, and M. Martinez-Sanchez, "A Micro-Fabricated Linear Array of Electrospray Emitters for Thruster Applications," *Microelectromechanical Systems, Journal of*, vol. 15, pp. 1260-1271, 2006.

[13] J. Darabi and K. Ekula, "Development of a chip-integrated micro cooling device," *Microelectronics Journal*, vol. 34, pp. 1067-1074, 2003.

[14] A. Richter and H. Sandmaier, "An electrohydrodynamic micropump," presented at the Micro Electro Mechanical Systems, 1990. Proceedings, An Investigation of Micro Structures, Sensors, Actuators, Machines and Robots., Napa Valley, 1990.

[15] J.-m. Wang and L.-j. Yang, "Electro-hydro-dynamic (EHD) micropumps with electrode protection by parylene and gelatin," *Tamkang Journal of Science and Engineering*, vol. 8, p. 231, 2005.

[16] H.-C. Wang, N. E. Jewell-Larsen, and A. V. Mamishev, "Thermal management of microelectronics with electrostatic fluid accelerators," *Applied Thermal Engineering*, 2012.

[17] H. T. G. Lintel van, F. C. M. Pol van de, and S. Bouwstra, "A piezoelectric micropump based on micromachining of silicon," *Sensors and Actuators*, vol. 15, pp. 153-167, 1988.

[18] J.-D. Moon, D.-h. Hwang, and S.-T. Geum, "An EHD gas pump utilizing a ring/needle electrode," *IEEE Transactions on Dielectrics and Electrical Insulation*, vol. 16, pp. 352-358, 2009.

[19] W. Qiu, L. Xia, X. Tan, and L. Yang, "The Velocity Characteristics of a Serial-Staged EHD Gas Pump in Air," *Plasma Science, IEEE Transactions on*, vol. 38, pp. 2848-2853, 2010.

[20] E. Moreau and G. Touchard, "Enhancing the mechanical efficiency of electric wind in corona discharges," *Journal of Electrostatics*, vol. 66, pp. 39-44, 2007.

[21] Q. Wei, X. Lingzhi, Y. Lanjun, Z. Qiaogen, X. Lei, and C. Li, "Experimental Study on the Velocity and Efficiency Characteristics of a Serial Staged Needle Array-Mesh Type EHD Gas Pump," *Plasma Science and Technology*, vol. 13, p. 693, 2011.

[22] I. Y. Chen, M.-Z. Guo, K.-S. Yang, and C.-C. Wang, "Enhanced cooling for LED lighting using ionic wind," *International Journal of Heat and Mass Transfer*, vol. 57, pp. 285-291, 1/15/ 2013.

[23] R. T. Huang, W. J. Sheu, and C. C. Wang, "Heat transfer enhancement by needle-arrayed electrodes - An EHD integrated cooling system," *Journal of Energy Conversion and Management*, vol. 50, pp. 1789-1796, 2009.

[24] Y. Otsubo and K. Edamura, "Viscoelasticity of a dielectric fluid in nonuniform electric fields generated by electrodes with flocked fabrics," *Rheologica Acta*, vol. 37, pp. 500-507, 1998/11/01 1998.

[25] M. Robinson, "Movement of air in the electric wind of the corona discharge," Research-Cottrell INC, New Jersey1960.

[26] B. Kim, S. Lee, Y. S. Lee, and K. H. Kang, "Ion wind generation and the application to cooling," *Journal of Electrostatics*, vol. 70, pp. 438-444, 2012.

[27] Y. P. Raizer, V. I. Kisin, and J. E. Allen, *Gas discharge physics* vol. 1: Springer-Verlag Berlin, 1991.

[28] J. Kuffel, E. Kuffel, and W. Zaengl, *High voltage engineering fundamentals*: Newnes, 2000.

[29] D. F. Colas, A. Ferret, D. Z. Pai, D. A. Lacoste, and C. O. Laux, "Ionic wind generation by a wire-cylinder-plate corona discharge in air at atmospheric pressure," *Journal of Applied Physics*, vol. 108, pp. 103306 - 103306-6, 2010.